Supplement of The Cryosphere, 17, 5241–5254, 2023
https://doi.org/10.5194/tc-17-5241-2023-supplement

The Cryosphere Open Access EGU

Supplement of

From atmospheric water isotopes measurement to firn core interpretation in Adélie Land: a case study for isotope-enabled atmospheric models in Antarctica

Christophe Leroy-Dos Santos et al.

Correspondence to: Christophe Leroy-Dos Santos (christophe.leroy@lsce.ipsl.fr)

Figure

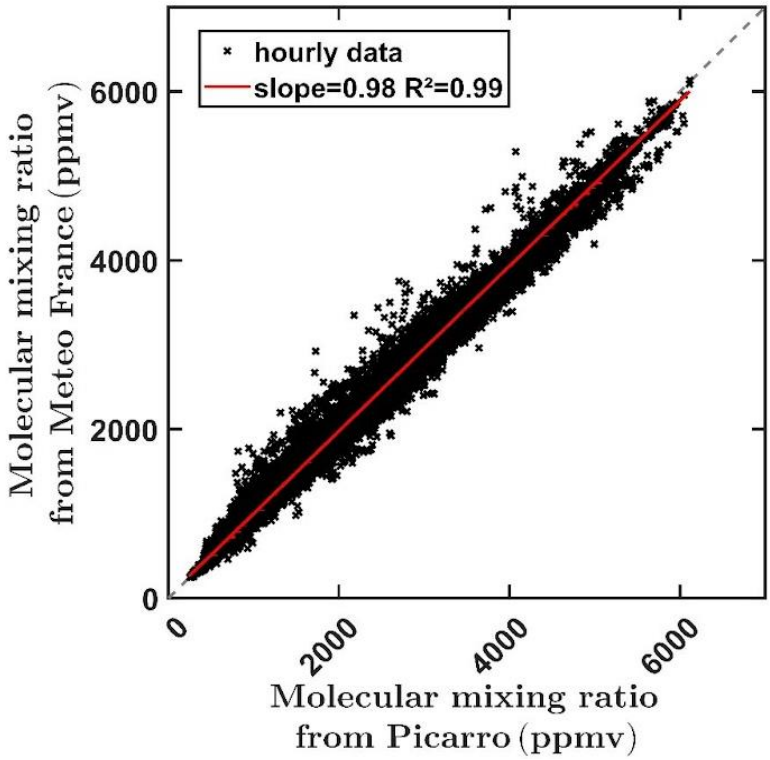

Figure S1: Molecular mixing ratio (ppmv) calculated from Meteo France sensors (estimated by the Magnus-Tetens approximations from temperature, surface pressure and relative humidity), versus molecular mixing ratio measured by Picarro. Red line is the linear relationship estimated from hourly averaged data.

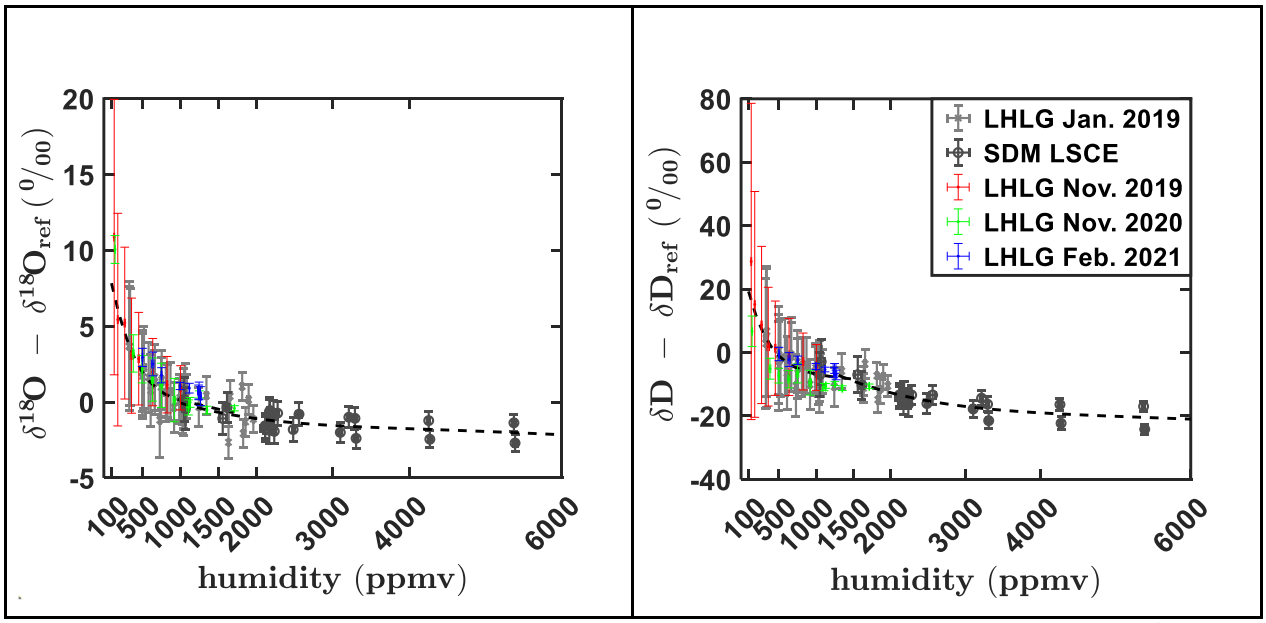

Figure S2: Humidity calibration curves showing the difference between the measured $\delta^{18}O$ (δD) and the reference $\delta^{18}O$ (δD) values (true value of the standard used: NEEM and FP5). Measurements have been averaged over 10 minutes and error bars represent the standard deviation over this time period (data resolution is 1 second for 2018, 2019 and SDM measurements, 1 minutes for 2020 and 2021 measurements).

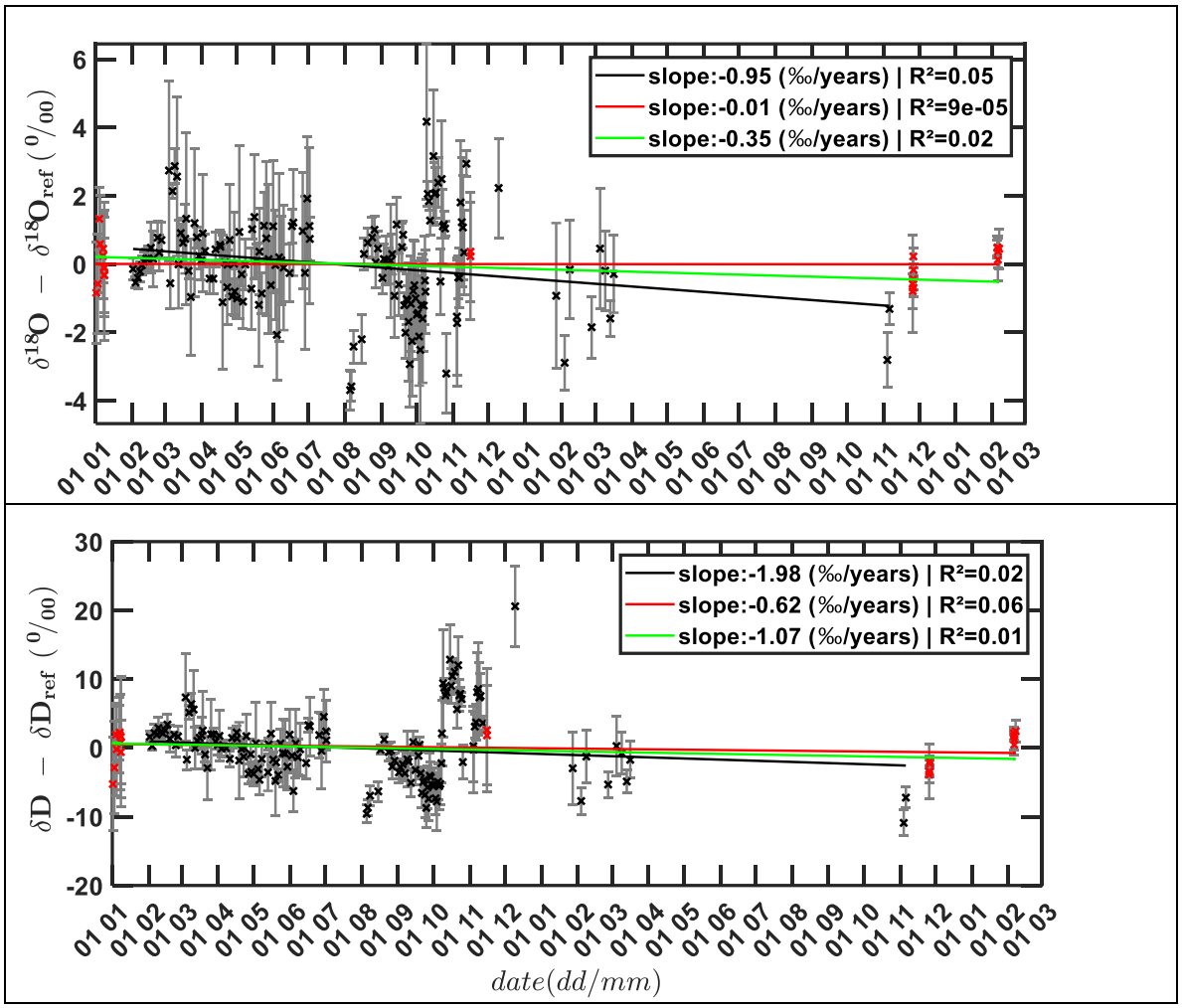

Figure S3: Mean linear drift estimation from different sets of data. Black crosses are routine measurements and red crosses are measurements made during humidity calibration sessions. Gray bars are the standard deviation associated with each measurement. Black (red) line is the linear drift estimated from routine measurements (humidity calibration sessions measurement). The green line is the linear drift estimated from both data series

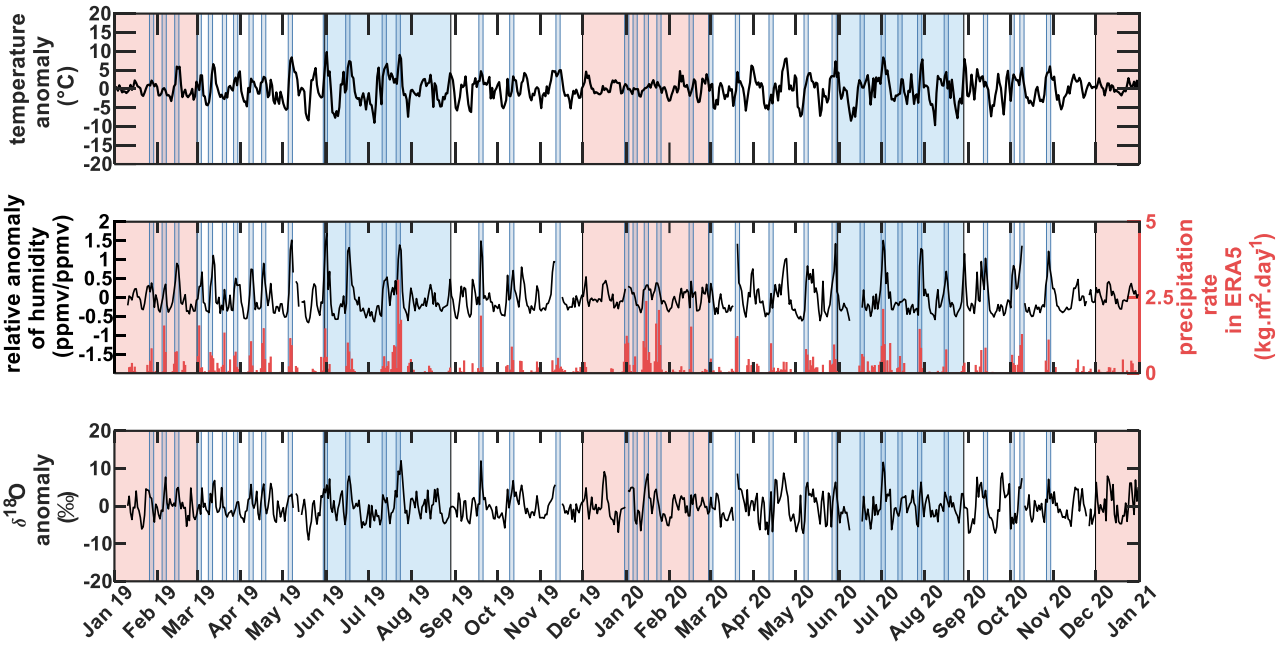

Figure S4: Anomalies of temperature, humidity and $\delta^{18}O$ over the 2019-2020 period. Anomalies are calculated as the difference between dailyvalue and 30-day running average.

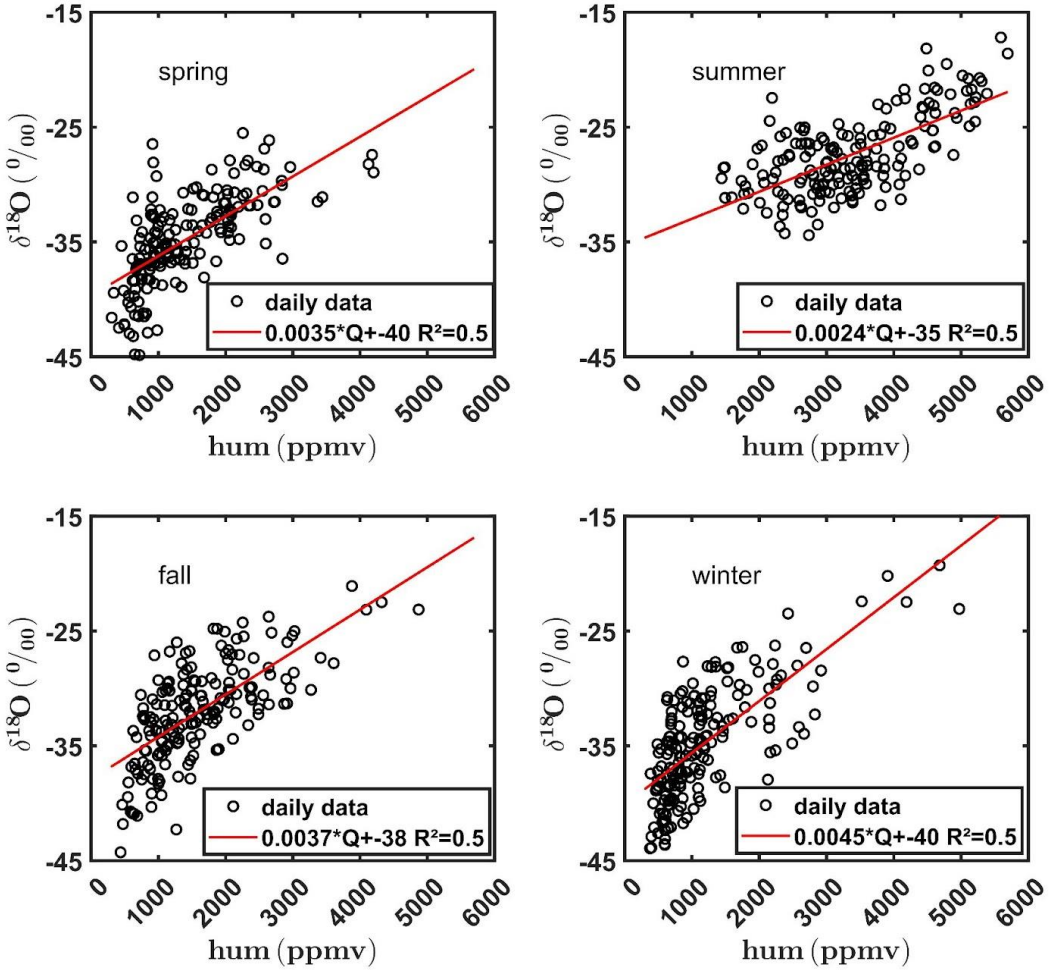

Figure S5: Observed relationships between $\delta^{18}O$ (‰) and humidity (ppmv) daily data according to the seasons(best linear fits in red).

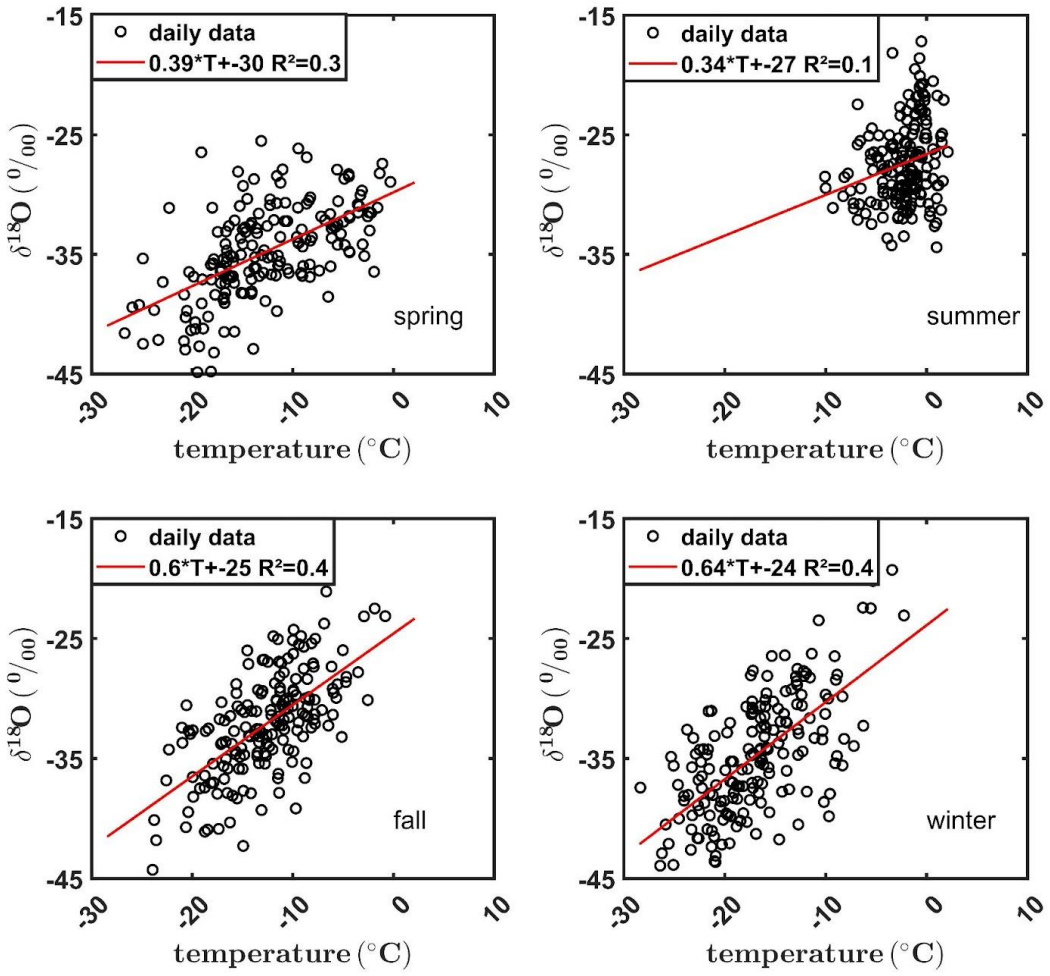

Figure S6: Observed relationships between $\delta^{18}O$ (‰) and 2-m temperature (°C) daily data according to the seasons (best linear fits in red; extrapolated over the -29°C – 2°C range).

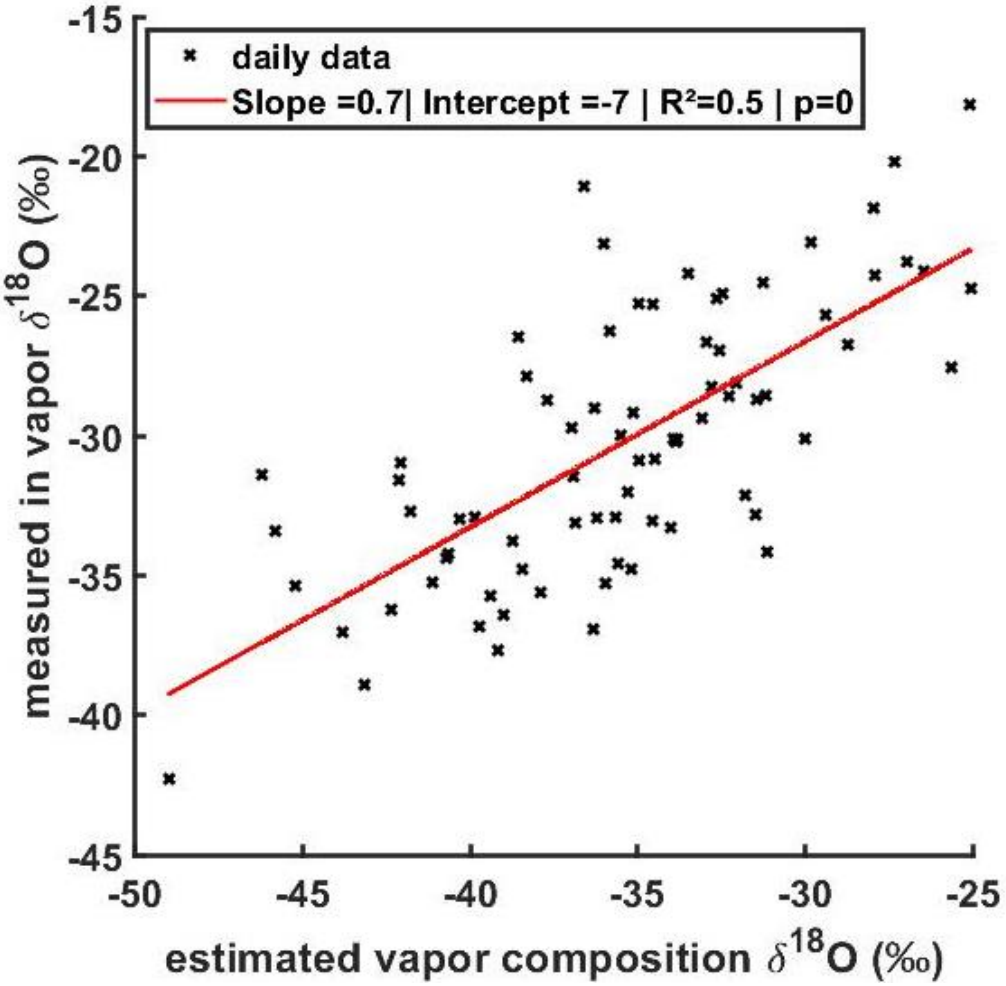

Figure S7: Relationship between the water isotopic composition of 1) the vapor measured at DDU station (daily average) and 2) the vapor which would be at equilibrium with precipitation samples assuming isotopic equilibrium (event-basis sampling). The red line is the linear regression on all precipitation events.

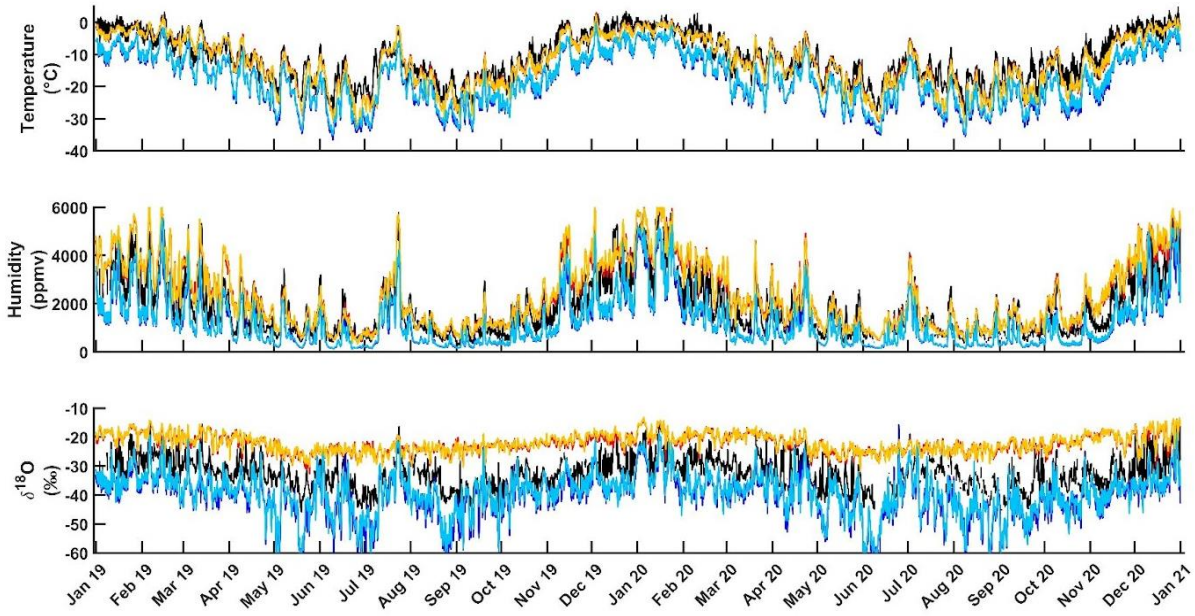

Figure S8: Meteorological and isotopic measurements at DDU at 6-hour resolution, in black. Panels from top to bottom: 1) 2m-temperature (°C) from Meteo France weather station, 2) humidity (ppmv) measured by the Picarro laser spectrometer; 3) $\delta^{18}O$ (‰) in water vapor. Colored lines are ECHAM6-wiso first level outputs (6-hour resolution) at DDU closest grid cells (colors as in Fig. 1).

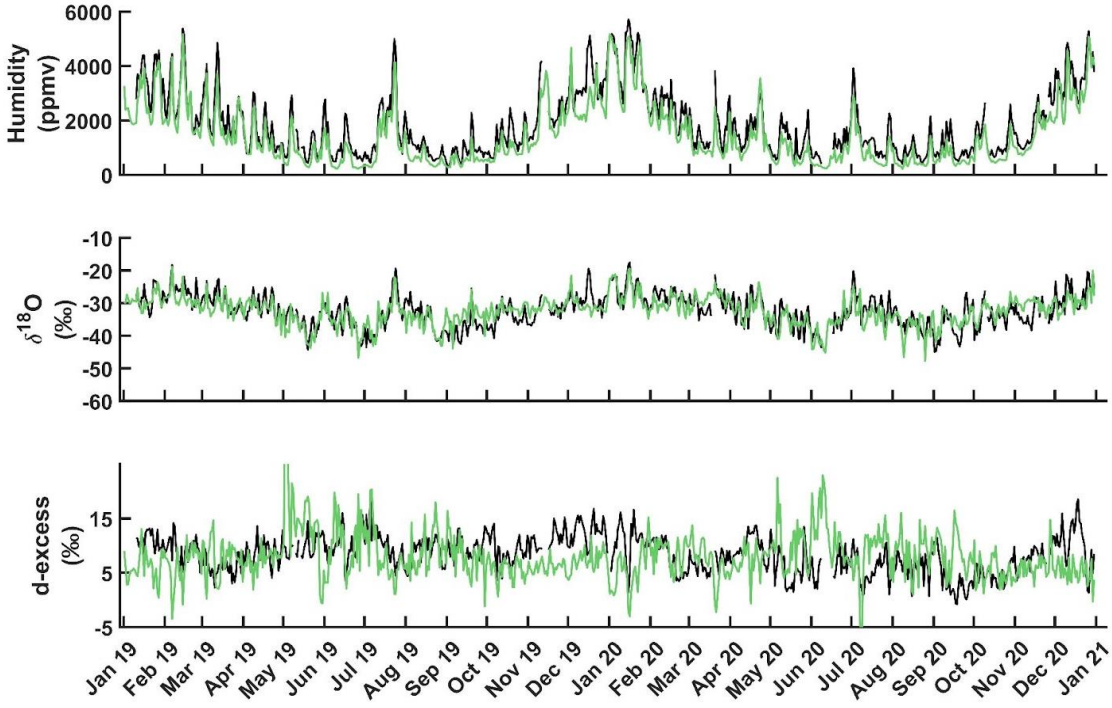

Figure S9: Comparison of humidity, δ18O and d-excess modeled by ECHAM6-wiso and measured at DDU station over the period 2019-2020. In black: Humidity and isotopic measurements at DDU at daily resolution. Panels from top to bottom: 1) humidity (ppmv) measured by the Picarro laser spectrometer; 2) $\delta^{18}O$ (‰) in water vapour 3) d-excess (‰) in water vapor. Green lines correspond to the ECHAM6-wiso combination of first level outputs (daily resolution) using isotopes optimisation (combination c), see main text).

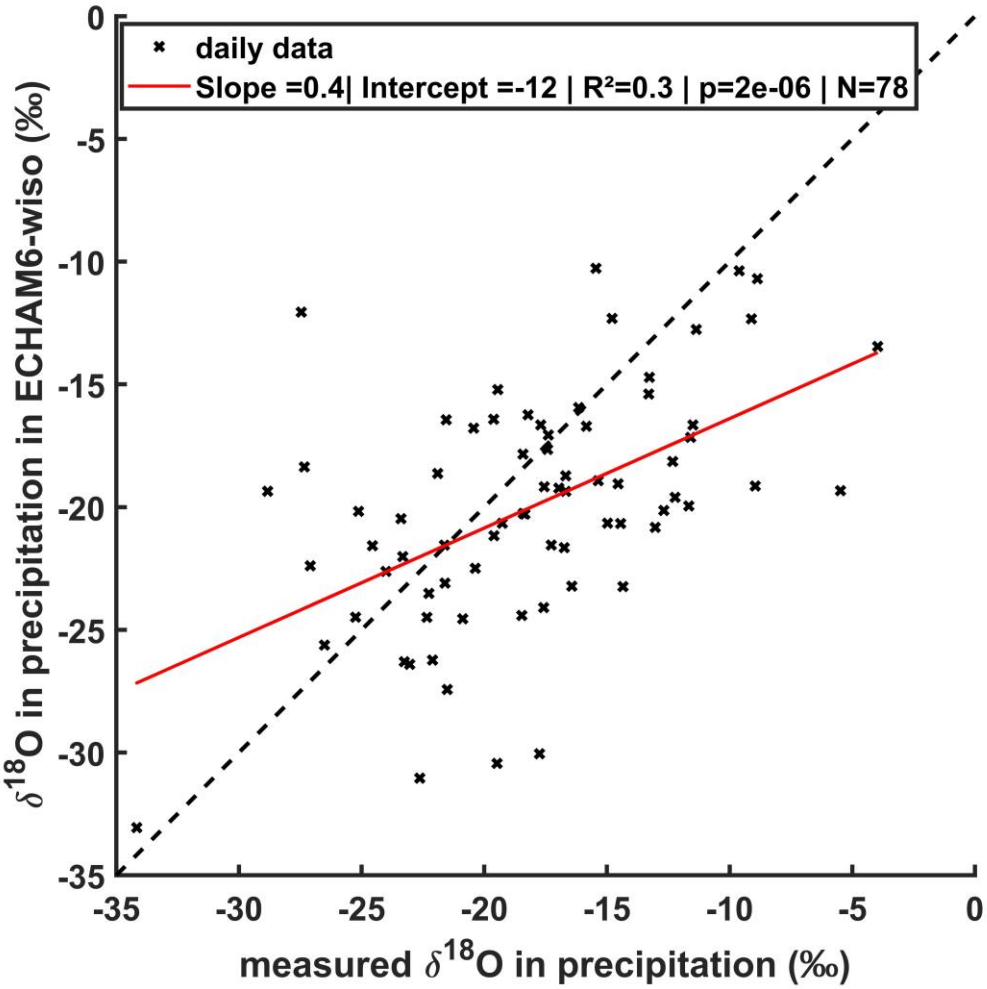

Figure S10: Relationship between the measured isotopic composition of precipitation at DDU and the daily output from ECHAM6-wiso grid combination (see text). Red line is the linear regression and the dashed line the 1:1 line.

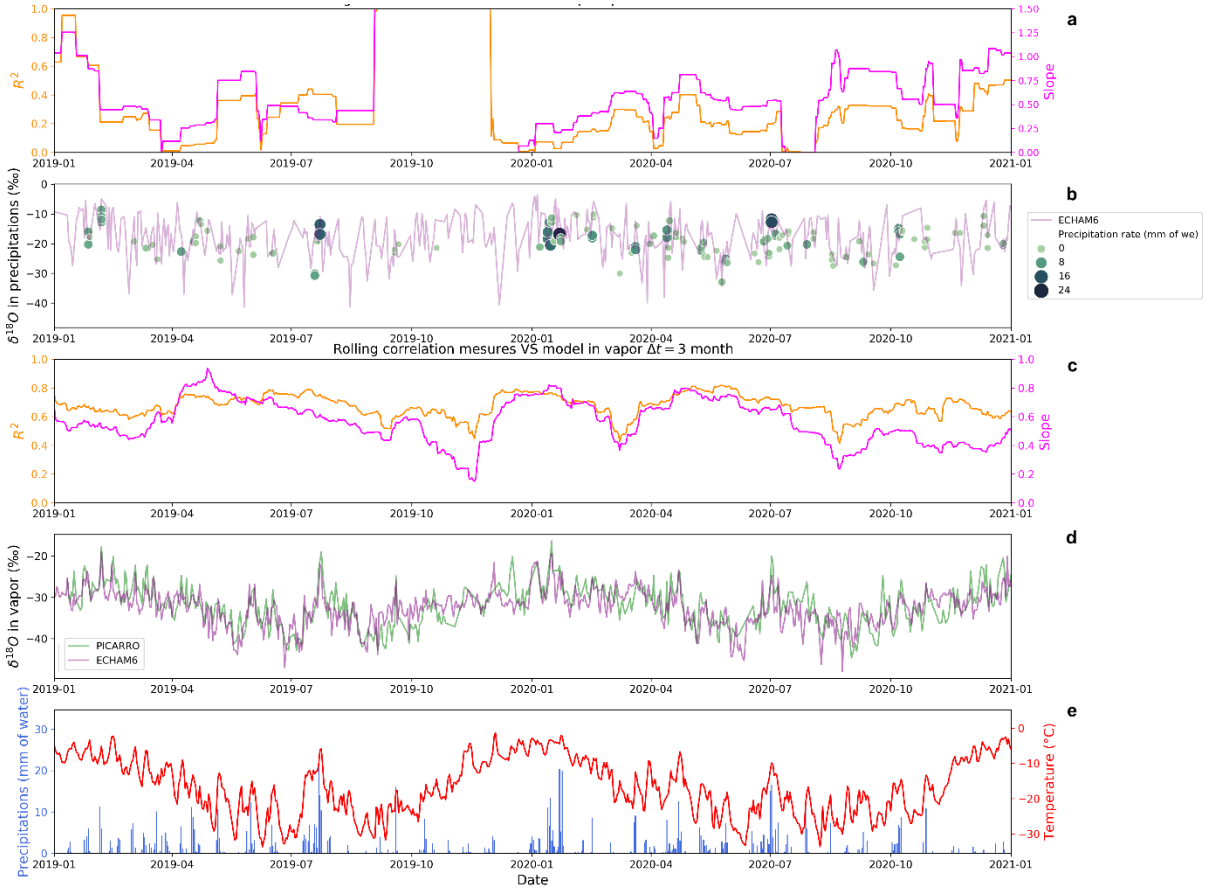

Figure S11: Temporal evolution of the relationship between modeled and measured $\delta^{18}O$ for the precipitation and the vapor water at DDU over the period 2019-2020. Panel a): Correlation (R^2, yellow) and slope (pink) between modeled and measured $\delta^{18}O$ in precipitation over a 3-month running window. Panel b): $\delta^{18}O$ of precipitation from the ECHAM6-wiso model (violet) and from sample measurements (green dots with size indicatiing the range of daily precipitation rate). Panel c): Correlation (R^2, yellow) and slope (pink) between modeled and measured $\delta^{18}O$ in the atmospheric vapor over a 3-month running window. Panel d): $\delta^{18}O$ of the vapor obtained from the ECHAM6-wiso model cell grid combination (violet) and from measurements (green). Panel e): Temperature (red) and daily precipitation amount (blue) from ERA5 reanalyse.

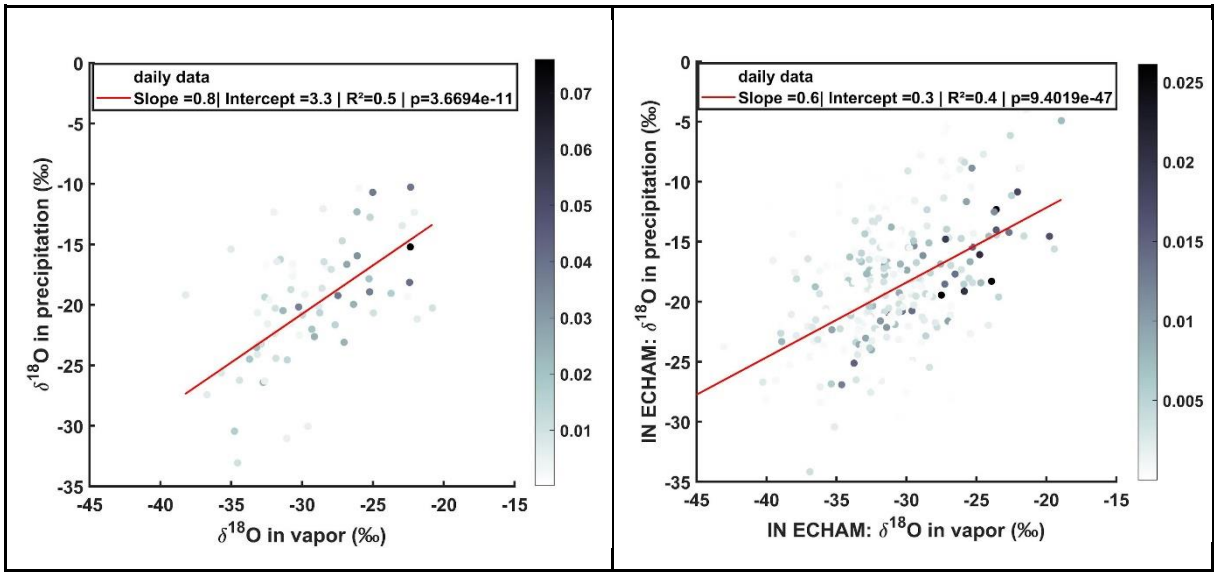

Figure S12: Relationship between the isotopic composition in vapor and in precipitation for measurement (left) and ECHAM6-wiso grid combination (right). Red lines are weighted linear fits from daily means. The dot colors indicate the amount of precipitation in m of we.

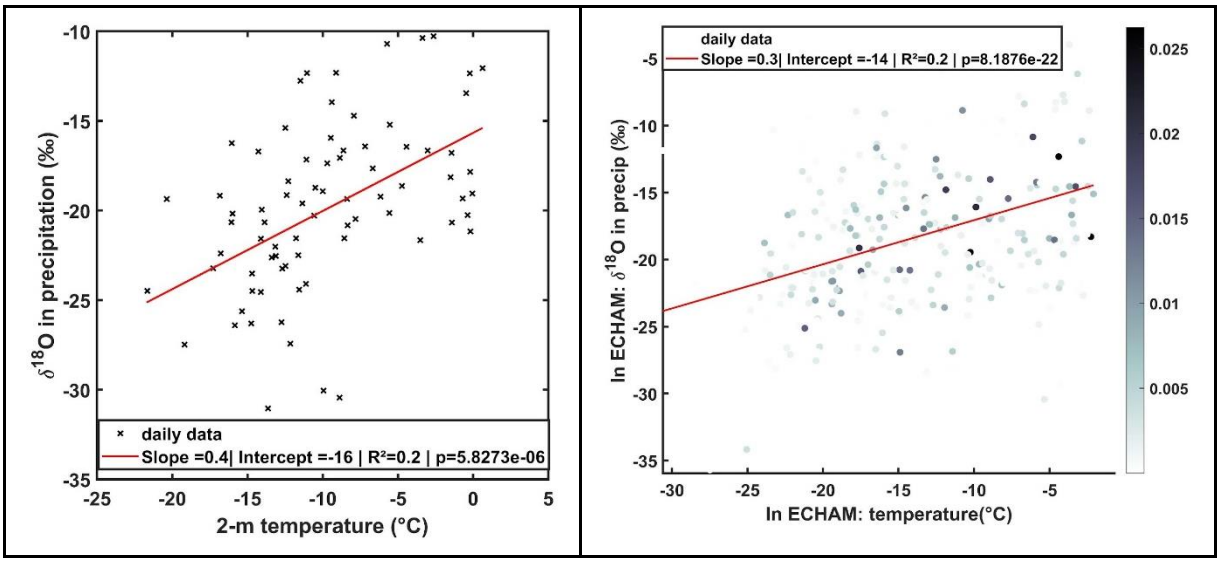

Figure S13: Water stable isotopic composition of precipitation ($\delta^{18}O$ in ‰) versus 2-meter temperature at DDU from measurements (left) and ECHAM6-wiso grid combination (over the 2019-2020 period). Linear fit in red. In ECHAM, we consider only precipitation with a total daily amount superior to 1kg.m-². Note also that we used the daily precipitation amount as a weight to compute the linear relationship (relationship with unweighted values: slope: 0.2, intercept: -15).

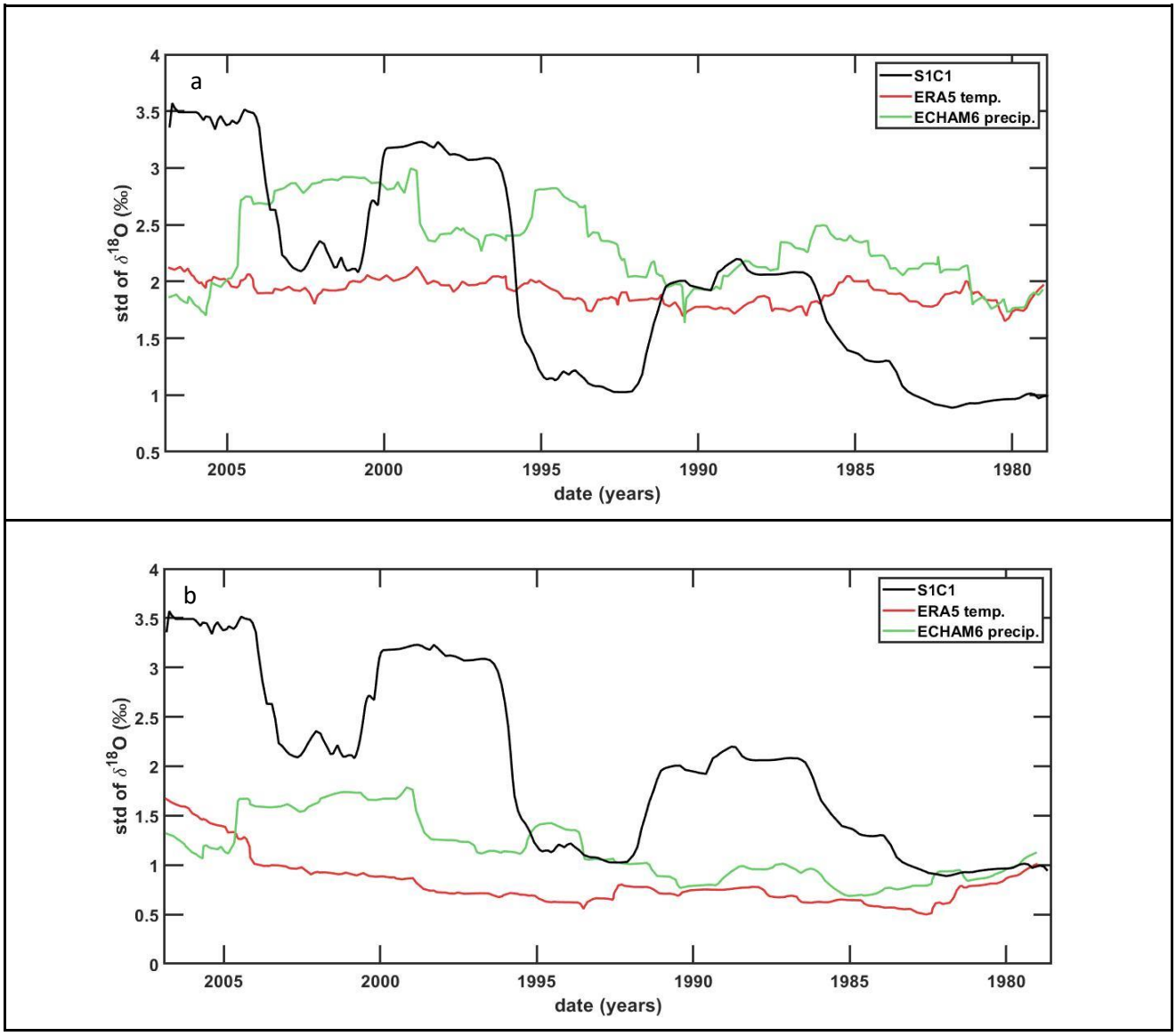

Figure S14: a: moving standard deviation over 40 samples (approximately 5 years) of S1C1 firn core (black), VFC-ERS5 (red) and VFC-ECHAM (green). b: Same as a taking into account diffusion in the VFC.

Table

Grid cells	Temp (°C)		T2m (°C)	Hum (ppmv)		Q2m (ppmv)	$\delta^{18}O$ (‰)		Temp Corr.		Hum corr		d18 corr		m.a.s.l.	mean topo (m.a.s.l.)
	mean	std	Mean	mean	std	Mean	mean	std	slope	R^2	slope	R^2	slope	R^2		
#1	-12.3	8.0	-12.1	2332	1368	2389	-22.2	2.9	1.1	0.9	1.1	0.9	0.3	0.3	68	0
#3	-12.5	7.9	-12.2	2357	1406	2431	-21.9	3.0	1.1	0.9	1.1	0.9	0.3	0.3	72	0
Oceanic	**-12.4**	**8.0**	**-12.2**	**2345**	**1386**	**2410**	**-22.1**	**2.9**	**1.1**	**0.9**	**1.1**	**0.9**	**0.3**	**0.3**	**70**	**0**
#2	-18.1	8.1	-19.0	1195	1024	1115	-39.4	7.3	1.1	0.9	0.8	0.9	1.1	0.5	712	645
#4	-17.7	7.9	-18.6	1237	1079	1162	-38.6	7.1	1.1	0.9	0.8	0.9	1.1	0.5	633	516
Continental	**-17.9**	**8.0**	**-18.8**	**1216**	**1050**	**1138**	**-39.8**	**7.1**	**1.1**	**0.9**	**0.8**	**0.9**	**1.1**	**0.5**	**673**	**581**

Table S1: Comparison of ECHAM6-wiso outputs and data. Left section of the table: models outputs for the first level of grid cells as defined in Fig. 1; for comparison, model outputs at 2m available for temperature and humidity are also given. Middle section of the table: correlation coefficient associated to linear regression between daily modelled outputs for each cell and data measured at DDU. Right section of the table: altitude of the grid cell center for the first level computed by ECHAM6-wiso, and surface altitude of the grid cell centers

		S1C1	ERA5 temperature			ECHAM6-wiso from precip.		
			wo diff.	diff.	diff. + strat.	wo diff.	diff.	diff. + strat.
$\delta^{18}O$ (‰)	mean	-18.7	-20.8	-20.8	-20.8	-17.5	-17.5	-17.5
	std	2.4	1.9	0.9	1.0	2.4	1.3	2.1

Table S2: Mean, standard deviation of isotopic composition of S1C1 and VFC records built from ERA 5 temperature and ECHAM6-wiso precipitation (see text). Calculations were performed for each VFC for different configurations: 1) isotopic diffusion 2) after isotopic diffusion 3) after isotopic diffusion and addition of simulated stratigraphic noise (results presented are the averages of 40 draws of white noise simulation).

Text

Text S1:

To assess the drift of the instrument, standard measurements (black crosses in Figure S3) was performed every 2 days with the humidity generator set at 1100ppmv during 40 minutes (1140ppmv measured on average). Some technical issues led us to select only 150 calibrations over the 2-year period. The results show a drift with decreasing $\delta^{18}O$ and δD values with time. Unfortunately, the data are very scattered and even sparse after the first year of installation of the instrument. The reason for this scattering is a problem with the humidity generator (bad drying procedure in the instrument) when it was working without human intervention. However, we could perform proper calibrations each year during the field summer seasons (red crosses). Because we are more confident with these measurements, we have only kept these series for the drift estimation.

Mean drift over the two-year period is hence estimated to 0.01 ‰/years and 0.6 ‰/years for $\delta^{18}O$ and δD, respectively. Because the drift is very small but associated with a high uncertainty, we decided not to correct our data series for mean annual drift but to associate a large uncertainty with $\delta^{18}O$ and δD. The latter is calculated as the 70^{th} percentile of the distribution of the 4 annual calibration during the summer season and results in 0.8 ‰ and 3.2‰, respectively. The new version of the LHLG (low-humidity level generator), installed in January 2022 at DDU, does not show any longer such a scatter in the routine drift calibrations; there is a good agreement between the drift inferred from this routine calibration and the drift calculated from the calibrations performed during the summer season showed in this study.

Text S2:

The Matlab VFC scripts (described in Casado et al. (2020)) use as inputs the 2m-temperature and the precipitation amount to create layers of firn core at a density

calculated through the Herron-Langway model (Herron and Langway, 1980) using forcing by surface temperature and accumulation. The temperature is converted in isotopic signal using a temperature to isotopes relationship (here estimated to be 0.44 $‰.°C^{-1}$ at DDU). The total precipitation amount of ERA5 and ECHAM6-wiso are rescaled to match the mean annual amount of accumulation at the drilling site (21.8 ± 6.9 $cm\ of\ w.e.year^{-1}$, Goursaud et al. (2017)). Here, the rescaling coefficient is 3.3 for ERA5 and 2.2 for ECHAM6-wiso (the total amount of snowfall in ERA5 and ECHAM6-wiso is larger than what has been actually accumulated at S1C1). VFC outputs are given with a resolution of 1 $mm\ of\ w.e$. Then, we resampled the VFCs using the density profile to match the resolution of S1C1 measurements (3cm of snow samples).

Text S3:

The effect of isotopic diffusion in the firn layers is estimated using the classical diffusion model from Johnsen et al. (2000) with addition of a depth-dependent diffusion length (Laepple et al., 2018). We use Matlab VFC scripts as described in Casado et al. (2020). As expected, diffusion smooths the signal (Figure 6) and $\delta^{18}O$ standard deviations in the VFCs become almost twice lower than in the S1C1 core (see Table S2 and Fig. S14).

Bibliography:

Casado, M., Münch, T., and Laepple, T.: Climatic information archived in ice cores: impact of intermittency and diffusion on the recorded isotopic signal in Antarctica, Clim. Past, 16, 1581–1598, https://doi.org/10.5194/cp-16-1581-2020, 2020.

Goursaud, S., Masson-Delmotte, V., Favier, V., Preunkert, S., Fily, M., Gallée, H., Jourdain, B., Legrand, M., Magand, O., Minster, B., and Werner, M.: A 60-year ice-core record of regional climate from Adélie Land, coastal Antarctica, The Cryosphere, 11, 343–362, https://doi.org/10.5194/tc-11-343-2017, 2017.

Herron, M. M. and Langway, C. C.: Firn densification: an empirical model, Journal of Glaciology, 25, 373–385, 1980.

Johnsen, S. J., Clausen, H. B., Cuffey, K. M., Hoffmann, G., Schwander, J., and Creyts, T.: Diffusion of stable isotopes in polar firn and ice: the isotope effect in firn diffusion, Physics of ice core records, 121–140, 2000.

Laepple, T., Münch, T., Casado, M., Hoerhold, M., Landais, A., and Kipfstuhl, S.: On the similarity and apparent cycles of isotopic variations in East Antarctic snow pits, The Cryosphere, 12, 169–187, https://doi.org/10.5194/tc-12-169-2018, 2018.